Raport Badawczy
Research Report

RB/5/2013

Emission data uncertainty in modeling urban air quality – a case study

P. Holnicki, Z. Nahorski

Instytut Badań Systemowych
Polska Akademia Nauk

Systems Research Institute
Polish Academy of Sciences

POLSKA AKADEMIA NAUK

Instytut Badań Systemowych

ul. Newelska 6

01-447 Warszawa

tel.: (+48) (22) 3810100

fax: (+48) (22) 3810105

Kierownik Zakładu zgłaszający pracę:
Prof. dr hab. inż. Zbigniew Nahorski

Warszawa 2013

Emission data uncertainty in modeling urban air quality – a case study

Piotr Holnicki [a], **Zbigniew Nahorski** [a]

[a] Systems Research Institute, Polish Academy of Sciences,
Newelska 6, 01-447 Warsaw, Poland

A decision support in air quality management connects several categories of the input data with an analytical model of air pollution. The model provides a quantitative assessment of environmental impact of emission sources in a form of pollutants' concentration/deposition maps, which in turn are used in supporting the planning actions. Due to the complexity of the forecasting system and the required input data, such an environmental prognosis and related decisions usually contain a substantial share of imprecision and uncertainty, especially in urban areas. The uncertainty in the model outcomes limits their credibility and usefulness in decision-making process. Therefore, the knowledge of the magnitude of model uncertainties is essential for decisions on emission abatement strategies. The main sources of uncertainty are commonly due to admitted meteorological and emission input data. This paper addresses the problem of urban-scale emission uncertainty, and related impact of this uncertainty on the forecasted model outputs. The computations are provided for the Warsaw Metropolitan Area, Poland, and encompass one-year forecast for the 2005 meteorological dataset. Detailed analysis of key uncertainty factors is based on the Monte Carlo technique where the regional scale CALPUFF model is the main forecasting tool for air pollution predictions.

Kewords: air quality, emission data, forecasting model, uncertainty analysis

1. Introduction: Modeling of air pollution transport

Air quality forecasting models and the more complex integrated assessment systems are recently developed for supporting decisions concerning air quality management and emission control policy, especially in an urban scale (Lim et al., 2005; Calori et al., 2006; Mediavilla-Sahagún & ApSimon, 2006; Oxley et al., 2009). The integrated systems aim to combine a classical pollution transport model with some economic, ecological, technological and other constraints and standards. Such a system, apart from the natural scenario analysis, gives also a

E-mail addresses: holnicki@ibspan.waw.pl ; nahorski@ibspan.waw.pl

possibility to formulate and solve optimization problems, which take into consideration environmental standards. This is a tool for a complex analysis of environment-oriented development strategies and their optimization (ApSimon et al., 2002; Holnicki, 2011; Carnevale et al., 2012). Irrespective of how complex such a system is, its main component is usually an air pollution dispersion model, which forecasts concentrations of polluting species in the atmosphere, while other modules are responsible for required constraints and limits. Uncertainty of the forecast is an important component to be considered when analysing decisions and their impacts.

In most deterministic models of air quality, the process of pollution transport is represented by a distributed parameter model, which is mathematically described by the set of advection-diffusion equations

$$\frac{\partial c_i}{\partial t} + \nabla \cdot \vec{U} c_i = \nabla \rho D \nabla (c_i / \rho) + R_i(c_1, c_2, \ldots, c_n, t) + S_i(\vec{x}, t), \qquad (1)$$

$$\text{for} \qquad i = 1, 2, \ldots, n,$$

in the time interval $(0, T)$, subject to appropriate boundary and initial conditions. Each equation in (1) corresponds to the *i*-th polluting compound, where c_i denotes its concentration; $\vec{U}$ – the wind field vector; D – the turbulent diffusion coefficient; R_i – the chemical transformation rates of pollutants; $S_i(x,t)$ – the emission/reduction rate of a specific pollutant at a given spatial and temporal location; ρ – the air density. Most of parameters depend on the actual meteorological conditions.

The exact form and structure of the model usually depends on its practical application, type of the polluting compounds which are considered, and the scale of modeling. A model usually takes into account the input data (emission field and meteorological data) as well as the main physical and chemical processes, which influence the transport in the atmosphere, and transformations of air pollution components models. However, various types of air quality

models may differ significantly in an approach to solving equations (1), and also to the scale of modeling. Spatial and temporal scales of the environmental impact of air pollution are correlated with and, moreover, they directly depend on the lifetime of pollutant (Jacobson, 2005; Holnicki, 2011), which can differ significantly between compounds. Depending on the adopted scale, there are corresponding categories of models: local, regional and global.

Estimation of the urban-scale pollution is a computationally sophisticated modeling problem due to complexity of emission field, and also due to complicated building orography and wind-field effects. Emission inventory of urban areas usually encompasses different categories of emission sources, characterized by specific emission parameters. Varieties of primary pollutants generate secondary compounds by means of chemical transformation processes. Due to high population density, urban air pollution exposure is a crucial factor associated with adverse health effects (Holnicki et al., 2010). In particular, many research indicate that a considerable harm in public health is caused by fine particulate matter, especially PM2.5 (Tainio 2009; Tainio et al., 2010).

To quantify possible ecological, economic or health benefits of emission abatement, estimates of incremental contributions of the respective group of emission sources to ambient concentrations is needed, with a reasonable accuracy. However, due to a very complex and multidisciplinary structure of such systems, there exist many sources of imprecision and uncertainty – both in modeling environmental effects of atmospheric pollution and also in the resulting regulatory decisions – such as: (a) input data (mainly emissions, boundary conditions, meteorological data), (b) structure of the mathematical model (simplifications and parameterizations of physical and chemical processes), (c) numerical scheme implementation. Most of uncertainty studies focus on uncertainties arising from the input data and the model parameterizations (Colvile et al., 2002; Warmink et al., 2010; Malherbe et al., 2011). Maxim and van der Sluijs (2011) address uncertainties introduced in all stages of modeling process as

well as in interactions with policy-makers. Implementations of operational models of air pollution (used as decision support tools) usually involve some specific simplifications or parameterizations and cannot completely characterize complex physical processes. For example, the height of the mixing layer and atmospheric stability are usually evaluated in course of an imprecise heuristic procedure. This is the source of conceptual uncertainty which is also reflected in the final results (Maxim & van der Sluijs, 2011). In particular, it relates to uncertainty in deriving trajectories in Lagrangian approach or sub-grid effects in Eulerian models (Sportisse, 2007). The problem of numerical scheme accuracy cannot be easily addressed, since the models are usually hard-coded and it is difficult to directly modify their parameters.

It is a common view in the literature, e.g. Russel & Denis (2000) or Sax & Isakov (2003) that emission field inventory is one of the main sources of uncertainty in modeling of air pollution dispersion. It is also known that official emission data are not accurate, due to inventory uncertainties of some categories of urban emissions. Emissions of major power plants of energy sector can be treated as relatively accurate because of well specified parameters of combustion process as well as those of the fuel used. On the other hand, emission data characterizing residential area or transportation system are usually based on aggregated and averaged information on fuel consumption and its parameters. These categories of data reflect neither the real temporal variability nor chemical constitution of polluting compounds and are remarkably uncertain. In complex uncertainty analysis, correlation between pollutants emitted by the same source (Page et al., 2003) have also to be taken into account.

There are several methods to assess uncertainties. The sensitivity of the mathematical model output to given model parameters can be derived using adjoint model equations and differential tools (compare Sportisse, 2007; Yang, 2011). On the other hand, the Monte-Carlo

methods are based on the analysis of the model outputs obtained from randomly generated sets of the input data (emissions, meteorological conditions, model parameters). This technique is relatively easy to implement and it is free from the limiting assumptions (see, for example ApSimon et al., 2002; Sax & Isakov, 2002; Malherbe et al., 2011, Yang, 2011). This approach is used in the analysis presented in this study.

2. Air pollution forecasts for Warsaw Metropolitan Area

The computations performed are related to forecasts and analyses of air pollution dispersion in the Warsaw Agglomeration. Their main aim was to evaluate the environmental impact of the dominant categories of emission sources and to estimate uncertainty of this forecast that is related to the uncertainty of emission field inventory. The regional scale, Gaussian puff dispersion model CALPUFF (Scire et. al., 2000) was utilized to simulate the air pollution transport and transformations within the domain.

The uncertainty analysis of emission data is particularly challenging in the case of urban or industrial areas (Colvile et al., 2002; Mediavilla-Sahagún & ApSimon, 2006; Oxley et al., 2009, Buchholz et al., 2013). The problem follows from a high spatial concentration of a large number of emission sources with different technological parameters (spatial characteristics, stack height, temperature and velocity of the outlet gasses), various fuel type used with diverse parameters, composition of polluting compounds, emission intensities, and as a consequence – different ranges of emission uncertainty.

These uncertainties should be taken into account in complex analysis, when the results are to be utilized in supporting regulatory decisions.

In the case of the presented Warsaw study the total emission field was decomposed into four basic categories, mainly according to emission parameters and intrinsic uncertainty. The assumed emission categories are the following:

• High point sources (mainly the energy sector) – uncertainty is relatively low, since both the combustion process and fuel parameters are well defined and stable. On the other hand, due to the high stacks, the modeling procedure should include the initial plume development near the source.

• Low point sources (other industrial sources) – higher uncertainty due to less precise technological characteristics as well as fuel parameters.

• Area sources (residential sector and distributed industrial sources) – high uncertainty; emission data are mainly estimated basing on fuel type used and fuel consumption.

• Linear sources (transportation system) – high uncertainty; emission data are estimated based on several traffic parameters (traffic modes and intensity, fuel used, its quality and consumption, age and technological parameters of cars).

The analysis covers a rectangle domain, approximately 30 km x 40 km of Warsaw Metropolitan Area (about 520 km^2 inside administrative borders) shown in Fig. 1. For computational purposes, the domain was discretized with a homogeneous grid with the step size h = 1 km. According to previous remarks, the emission field was categorized into the following four classes:

• 16 high point sources (power/heating plants),

• 1002 low point sources (industry),

• 872 area sources (residential sector),

• 1157 linear sources (transportation).

The location of the point sources is defined by their geographical coordinates, while the area and linear sources are characterized by the respective, spatial mesh elements 1 km x 1 km that coincide with the domain discretization grid. Computations take into account temporal variability of the meteorological and emission input data, where the assumed step-size of time resolution is $\tau = 1h$.

The list of the main primary and secondary pollutants considered in the study is presented below as Table 1. The composition of emitted species depends on the source category. In particular, the point sources emit mainly sulfur oxides, nitrogen oxides, particulate matter, PPM_{10} and $PPM_{2.5}$ and, for certain particular sources, also BaP and some heavy metals. Area and linear sources may emit most of the listed compounds, but only linear sources are responsible for secondary emission of particulate matter, PPM_{10}_R and PPM2.5_R (total amount of dust particulates re-suspended due to the road traffic).

Concentrations of particulate matter (PM_{10} or $PM_{2.5}$) are calculated as a sum of the primary pollutions emitted by all categories of sources (PPM_{10} or $PPM_{2.5}$), the pollutions coming from the secondary, re-suspended emissions of the linear sources (PPM_{10}_R or $PPM_{2.5}$_R) and the concentrations of the secondary pollutants, like the sulfate and nitrate aerosols, which are also components of particulate matter (see Table 1).

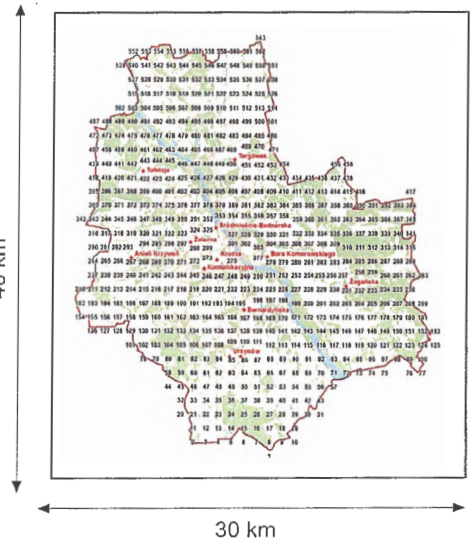

Model: CALPUFF

Emission sources:

high point sources	-	16
other point sources	-	1002
area sources	-	872
linear sources	-	1157

Emission & meteo data:
year 2005, (1h time step)

Spatial discretization:
1 km x 1 km

Receptors:
563 (grid 1 km x 1 km)

Fig. 1. The computational domain, the main parameters, the receptors' location.

Table 1. Polluting species considered (primary and secondary).

Emission / primary pollution	Secondary pollution
SO_2 (sulfur dioxide))	$SO_4^{=}$ (sulfate aerosol)
NOx (nitrogen oxides)	NO_3^{-} (nitrate aerosol)
	HNO_3 (nitric acid)
PPM_{10} (primary PM, diameter ≤ 10 μm)	
PPM_{10}_R (PPM_{10} re-suspended by road traffic – secondary emission)	$PM_{10} = PPM_{10}+PPM_{10}$_R+ $SO_4^{=}$ + NO_3^{-}
$PPM_{2.5}$ (primary PM, diameter ≤ 2.5 μm)	
$PPM_{2.5}$_R ($PPM_{2.5}$ re-suspended by road traffic – secondary emission)	$PM_{2.5} = PPM_{2.5}+PPM_{2.5}$_R+ $SO_4^{=}$ + NO_3^{-}
BaP (Benso [a] Pyren)	
Ni (nickel)	
Cd (cadmium)	
Pb (lead)	
PAH (Polycyclic Aromatic Hydrocarbons)	

The emission field encompasses sources located inside administrative borders and also some main sources outside Warsaw, but located in the computational domain, as shown in Fig. 1. The trans-boundary inflow forms the background for the pollutants originated from the local sources. The inflowing pollutions are taken into account as the boundary conditions for CALPUFF simulations and are based on the European scale EMEP model predictions (spatial resolution 50 km x 50 km). Results discussed in the following sections concern some accuracy and uncertainty estimates.

3. Simulation

Figure 2 contains two exemplary presentations of the modeling results (ArcMap/ArcInfo instrumentation is used). This figure consists of two maps presenting the annual mean concentrations of SO_2 and PM_{10} at the receptor points (only influence of the local Warsaw

sources is shown), including the relative share of emission categories in the total concentration. As shown in the next section, it is an important factor in quantitative uncertainty assessment. Each map is composed of five sectors: the central district of the city and four peripheral (border) districts.

Sulfur dioxide in Warsaw mainly comes from fuel combustion in point and area sources, while PM_{10} is strongly related to linear sources of transportation system. Annual mean concentrations of SO_2 are definitely below the admissible level, and the spatial changes of concentration are minor within the domain (compare Fig. 2a). All four early mentioned emission categories contribute to the final SO_2 pollution with the dominating share of the point sources. More significant contribution of the high point sources can be noticed in Northern districts (N-W and N-E), situated near the administrative city borders. It follows, first of all, from the stack height of the main Warsaw power/heating plants (100 – 300 m), so that their influence close to the ground can be observed only in some distance from the source. Moreover, high stacks of the heating plants which are all equipped with the effective filtering installations. Another reason are the dominating S and S-W wind directions in the analyzed 2005 period, as shown in Fig. 3.

In the case of the particulate matter (both PM_{10} and $PM_{2.5}$) contribution of linear sources dominates, and the pollution spatial variability within the domain is very significant (compare Fig. 2b). In particular, the PM_{10} concentrations in the city center are several times higher than those in peripheral districts; high concentrations are also observed along the arterial streets. At the same time, the share of emission categories varies spatially, and the contribution of area sources as well as local point sources considerably increases in the peripheral districts. This is rather a local effect and is recorded mainly in the neighborhood of S-W city borders of Warsaw, where a small (several per cent) contribution of the low point sources can be noticed. On the other hand, the contribution of the high point sources is

practically negligible within the whole domain, as mentioned above. The dominating contribution to particulate matter comes from the car traffic, including heavy truck traffic, also in central districts of the city.

A similar characteristics of the dominating impact of linear sources (mainly car traffic) and practically negligible contribution of high point sources, is also observed for NOx pollution (presented in more details in Section 5). For this pollutant there are also very significant differences in concentration between central (very high values) and peripheral districts (relatively low values).

Vicinities of arterial streets are also the regions of high nitrogen oxides concentrations, in spite of relatively coarse space discretization used for simulation.

In order to assess accuracy of model forecasts in this study, the calculated annual average concentrations of the main polluting compounds were compared (including the inflow from the surrounding areas) with measurements (locations of the main measurement stations are shown inFig. 1). For the year considered, air quality measurements were performed by several monitoring stations (automatic or manual). The number of observed pollutants differs in the stations, being quite limited in some cases. Table 2a shows comparison of the measured and computed average concentrations for the main gaseous pollutants: NOx, PM_{10}, SO_2 and heavy metals (Table 2b): Pb, Cd, Ni, depending on the observation point and the polluting compound.

a)

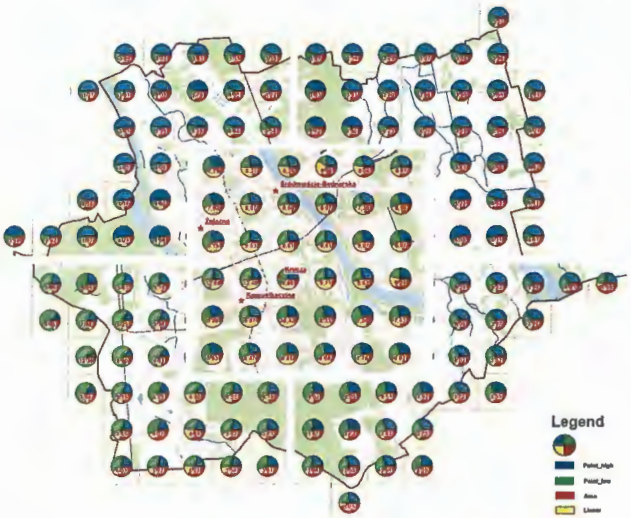

b)

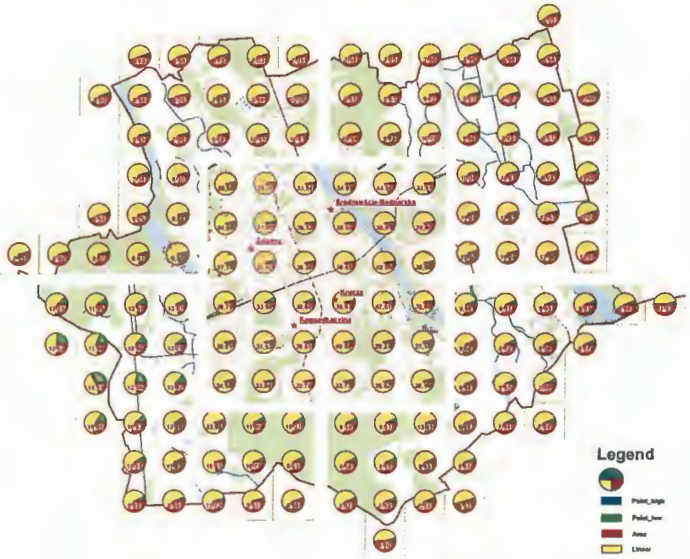

Fig. 2. The share of emission categories (annual mean concentrations): a) SO_2 and b) PM_{10}.

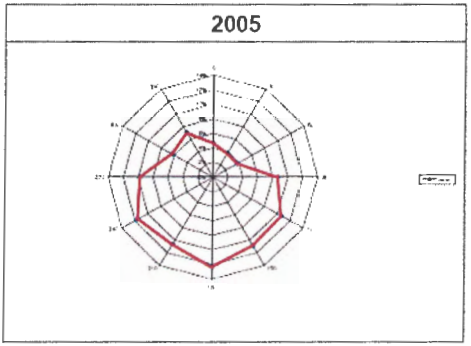

Fig. 3. Annual wind rose for Warsaw.

Moreover, a graphical presentation of calculated concentrations versus measurements is shown for those pollutants, for which a sufficient number of observations is available (9-13 for PM_{10}, NOx, SO_2). Figure 4 presents comparison of the predicted, year average concentrations with the measurement values registered at the monitoring stations for the particulate matter (PM_{10}), nitrogen oxides (NOx) and sulfur dioxide (SO_2). The dashed lines determine the domain where the ratio of computed and measured values do not exceed the factor of 2 (usually applied in comparison of modeling and observed atmospheric pollution data). The predicted PM_{10} and SO_2 concentrations follow the measured values sufficiently well. However, many of NOx predictions are underestimated. This follows from the fact that nitrogen oxide pollution is mainly produced by car traffic and the values are shown as averaged on the grid element (1km x 1 km), while measurements of monitoring stations often represent point-wise values near the roads axis.

Table 2a. Comparison of the modeled and measured air pollution concentrations.

No.	Monitoring station	PM_{10} [µg/m^3]			NO_x [µg/m^3]			SO_2 [µg/m^3]		
		Modeled	Measured	Error [%]	Modeled	Measured	Error [%]	Modeled	Measured	Error [%]
1	Białobrzeska	33	29,5	11,9	-	-	-	-	-	-
2	Bednarska	42	34,1	23,2	46,7	56,8	-17,8	-	-	-
3	Komunikacyjna	40	51,7	-22,6	51,2	76,2	-32,8	13,9	9,8	41,8
4	Żelazna	34	32,9	3,3	45,6	36,3	25,6	15,6	9	73,3
5	Krucza	43,2	41,7	3,6	31,3	35,7	-12,3	9,8	9,3	5,4
6	Ursynów	32	32,8	-2,4	27,5	19,2	43,2	9,3	8,8	5,7
7	Nowoursynowska	33,5	42,2	-20,6	23,1	25,6	-9,8	9,5	10,5	-9,5
8	Tołstoja	22	37,2	-40,9	35,2	43,1	-18,3	12,1	11,8	2,5
9	Targówek	31,6	31,9	-0,9	-	-	-	-	-	-
10	Anieli Krzywoń	24	31,3	-23,3	-	-	-	-	-	-
11	Bernardyńska	33	21,2	55,7	-	-	-	10,4	8,7	19,5
12	Bora-Komorowskiego	40,5	34,9	16,0	-	-	-	-	-	-
13	Żegańska	27	39,2	-31,1	-	-	-	-	-	-
14	Puszczy Solskiej	-	-	-	26,4	34,1	-22,6	10,6	12,9	-17,8
15	Porajów	-	-	-	19,6	24,1	-18,7	-	-	-
16	Lazurowa	-	-	-	-	-	-	10,1	11,2	- 9,8

Table 2b. Comparison of the modeled and measured air pollution concentrations.

No.	Monitoring station	Pb [ng/m^3]			Ni [ng/m^3]			Cd [ng/m^3]		
		Modeled	Measured	Error [%]	Modeled	Measured	Error [%]	Modeled	Measured	Error [%]
1	Bernardyńska	22,7	12	89,2	2,3	6,1	-62,3	0,73	0,45	62,2
2	Żelazna	24,5	34	-27,9	1,8	1,5	20,0	0,65	0,7	-7,1
3	Żegańska	20,2	41	-50,7	3,2	2,8	14,3	1,10	0,9	22,2
4	Anieli Krzywoń	18,3	47	-61,1	-	-	-	-	-	-

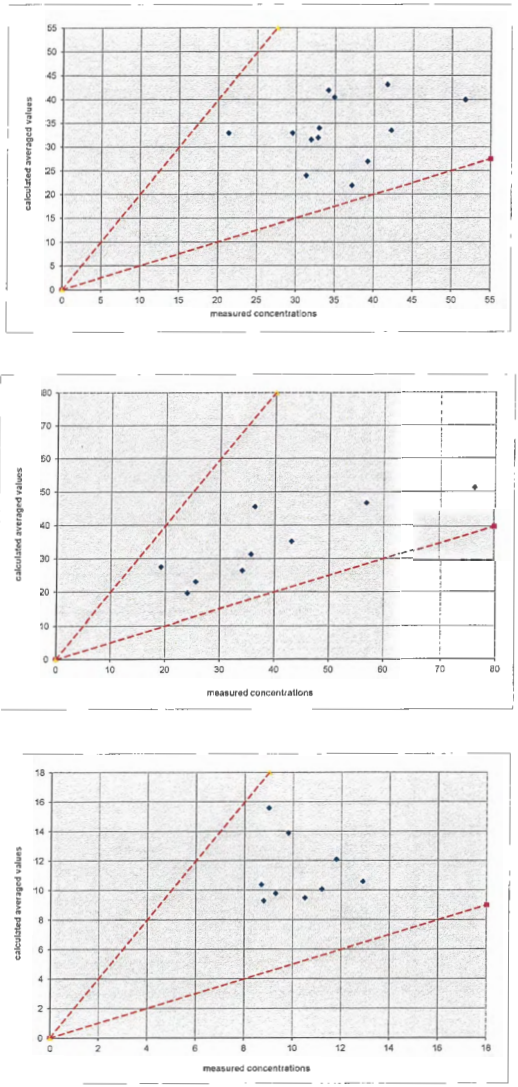

Fig. 4. Calculated vs. measured concentrations [$\mu g/m^3$]: (a) PM_{10}, (b) NOx, (c) SO_2.

4. Uncertainty analysis

In order to assess uncertainty of the concentration forecasts related to emission uncertainty, Monte Carlo algorithm was applied (Sax & Isakov, 2003; Holnicki et al., 2010; Yang, 2011). For each emission source 2000 randomly generated sets of emission volumes were prepared, according to the assumed uncertainty range. To avoid unrealistic emissions, a correlation was established between the emission intensity of the individual compounds within a source (see Page et al., 2003; Holnicki et al., 2010).

Table 3 presents general uncertainty ranges which were accepted for 4 categories of emission sources (based on expert opinions). Normal distributions of the input emission data were assumed.

Table 3. Assumed uncertainty range depending on the emission category (95% confidence interval).

Pollutant	Emission sources			
	High point	Other point	Area	Linear
SO_2	± 15%	± 20%	± 30%	± 30%
NOx	± 20%	± 30%	± 40%	± 40%
PPM_{10}	± 25%	± 40%	± 40%	± 40%
$PPM_{2.5}$	± 25%	± 40%	± 40%	± 40%
PPM_{10}_R	–	–	–	± 40%
$PPM_{2.5}$_R	–	–	–	± 40%
BaP	± 30%	± 40%	± 50%	± 50%
Ni	± 30%	± 40%	± 50%	± 50%
Cd	± 30%	± 40%	± 50%	± 50%
Pb	± 30%	± 40%	± 50%	± 50%
PAH	–	–	± 50%	± 50%

Some selected results of uncertainty analysis are presented for 5 main pollutants which characterize urban air quality, namely NOx, PM_{10}, $PM_{2.5}$, Pb, SO_2. They directly originate from the urban transportation system as well the local point and area sources. Figure 5, prepared by using ArcMap, shows distribution of annual mean concentrations of SO_2 and PM_{10} in the central district of the city. The bars refer to the annual concentration of the

selected pollutant at a given receptor. The colored sections in the top part of the bar represent the percentiles of emission uncertainty, with the colors coded according to the legend. This type of graphical presentation of uncertainty has a qualitative and approximate character.

A more precise characteristic of uncertainty for any selected receptor is illustrated in Figure 5 for receptor 273 (SO_2 concentration) and receptor 275 (PM_{10} concentration), see Figure 1 for identification of the receptor numbers. In this case one can obtain graphs of the empirical cumulative distribution curve, the empirical density function and the standard "box plot" for uncertainty distribution. The mean concentrations of PM_{10} at the same receptors are about 4–5 times higher than the respective values for SO_2 (in $\mu g/m^3$), compare graphs in Figures 5a and 5b. Moreover, for receptors presented in this figure, the resulting uncertainty range of PM_{10} is also much wider than the corresponding value for SO_2. The factor which determines uncertainty range is the location of the receptor, which is connected with relative contributions of individual emission sources of different categories in the measurements.

Figure 6 compares distribution of the standard deviation (left) and the relative uncertainty range (right) versus the annual mean concentrations calculated at 563 receptor points (as shown in Figure 1) for NOx, PM_{10}, SO_2 and Pb, respectively. The relative uncertainty range at a receptor point is calculated as a ratio $(c_{97.5} - c_{2.5})/c_M$, where $c_{2.5}$ is the 2.5 percentile concentration value, $c_{97.5}$ is the 97.5 percentile value, and c_M is the mean value. In all cases the values of standard deviation increase faster than linearly as a function of the mean concentration. A more cluster-shaped distribution of SO_2 standard deviation is a result of a relatively homogeneous spread of SO_2 concentration over the Warsaw domain, with the mean values much below the admissible levels. This follows from the dominating share of point sources in the heating system; very high stacks of plants in the district central heating system mainly affect very distant receptors (often outside the domain), while small point sources of individual heating are mainly active in peripheral districts. Moreover, the outside inflow of sulfur dioxide is a substantial part of the total SO_2 pollution.

a)

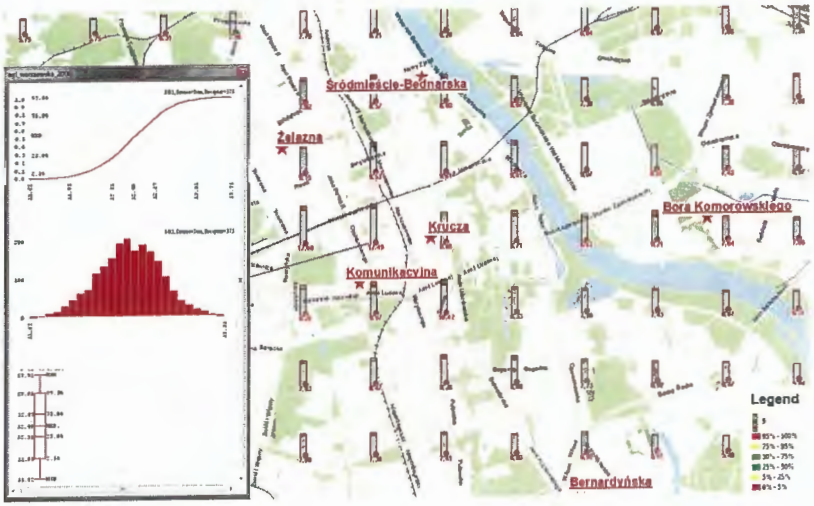

b)

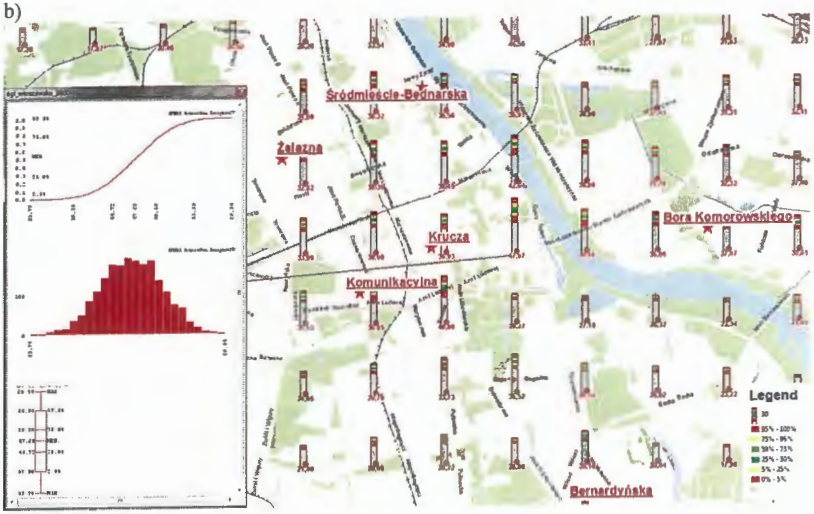

Fig. 5. Annual mean concentrations at receptors and their uncertainty distributions for: a) SO_2 (receptor 273) and b) PM_{10} (receptor 275).

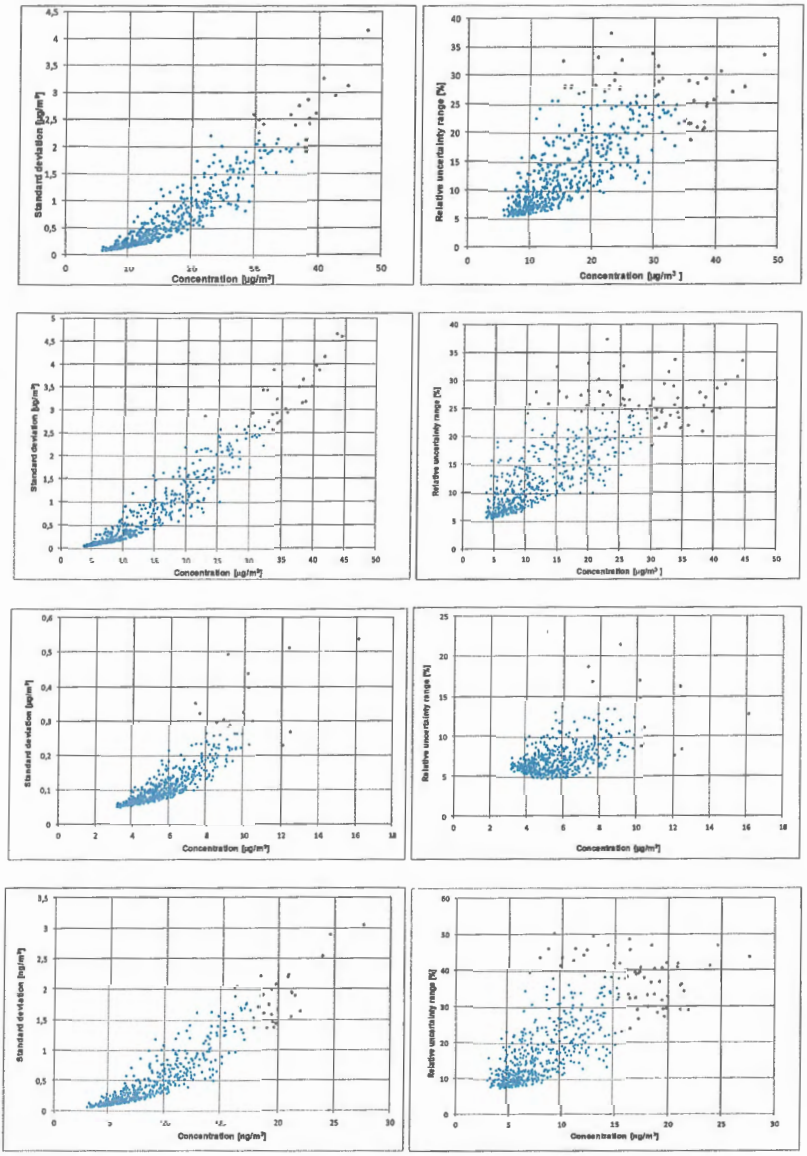

Fig. 6. Standard deviation (left) and relative uncertainty range (right) versus concentration level in 563 receptors. From top to bottom: PM_{10}, NOx, SO_2, Pb, respectively.

Other details related to uncertainty problem are explained in Figure 7, which comprises the pairs of maps, presenting spatial distribution of the mean concentration (left) and relative uncertainty level (right), for NOx, PM_{10}, $PM_{2.5}$, SO_2, Pb, respectively. It can be seen that typical traffic related species, like NOx, PM and Pb, show high uncertainty in vicinity of the main roads, with local maxima in surroundings of crossroads, which are determined by the share of emission sources affecting the receptor.

General similarity of both types of maps is caused mainly by the transportation induced pollution, such as particular matter, nitrogen oxides or lead. In Figure 7 (left) their high spatial diversification can be noticed, with the maximum values in the city center and near the arterial streets. This spatial diversity is much more apparent in uncertainty maps, where high values reflect quite well the traffic network's structure and the main crossroads. This effect is seen mainly for NOx, PM_{10}, and Pb. In these cases, high uncertainties are correlated with concentration values, but actually depend on the receptor's location, which decides on the relative share of contributing emission categories and the number of individual emission sources affecting this receptor point. A specific coincidence of these factors leads to extreme values of the overall uncertainties in some receptors.

On the other hand, pollutants which are not dominated by the transportation sources (for example SO_2) are more uniformly distributed over the domain and the corresponding uncertainties are rather low. In this case high uncertainty levels reported at some receptor points do not coincide with high concentrations, and are caused by other factors.

To analyze the problem in more details, the concentrations and the corresponding uncertainty levels are considered for two selected receptors, 136 and 156 (compare Figure 1). The first one characterizes a typical transportation affected spot (intersection of main roads), the other one is mainly affected by local area sources. It can be seen, referring again to Figure 7 (right), that uncertainties of the typical traffic related species, like NOx, PM_{10}, $PM_{2.5}$, and Pb, are high in a vicinity of this crossroad (receptor 136). It is seen from Figure 8 (left) that linear sources have a dominating contribution in this case. But apart the emission category, a

number of individual sources which substantially contribute to the point, is another important factor influencing uncertainty. Generally, due to the averaging process, increasing number of emission sources that substantially contribute to the receptor, cause decrease of the total relative uncertainty (the standard deviation for n equally contributing sources is proportional to $1/\sqrt{n}$). So, the less sources contribute to the pollution level, the higher relative uncertainty may be expected. Simultaneously, an unbalanced contribution of individual sources (for example, strong domination of one uncertain emission source) generally increases total uncertainty.

A general quantification of the last property is also possible, but below it is assessed qualitatively basing on Figure 8, which indicates the dominating individual sources responsible for about 60% of the overall pollution (concentration) assigned to receptor 136. It can be seen that for the highly uncertain NOx (~35%), Pb (~40%) and $PM_{2.5}$ (~30%) there are only four contributing sources of approximately equal uncertainty, with dominant contribution of one of them. Their uncertainties are on the level of uncertainties of pollutant emissions. On the other hand, in the case of SO_2 (Figure 8, bottom) a more balanced contribution of four emission categories is observed, with about 15 individual emission sources in total, most of them influencing considerably the final pollution. The total relative uncertainty level for SO_2 forecast is considerably lower for the receptor considered (~12%).

Characteristic of receptor 156 (compare its location in Figure 1) is completely different. As can be seen from Figure 7 (right), uncertainties of typical traffic-related pollutants (NOx, PM_{10}, Pb) are there relatively low, but the maximal (over the entire domain) values are obtained for SO_2 and $PM_{2.5}$. This again can be explained by looking at Figure 9, which presents the relative share of emission categories as well as the number of individual sources mainly contributing to the total concentration measured at this receptor. The influence of the area sources is dominating in this case, since this district comprises residential area with a number of small dwelling-houses with local coal-based heating/cooking installations. On the other hand, a substantial share of linear emission sources can be noticed for all NOx,

PM_{10}, Pb with exception of sulfur dioxide and medium contribution in case of $PM_{2.5}$. It can be seen in Figure 9 (right) that only 5 individual sources contribute to SO_2 and $PM_{2.5}$ pollution, and in these two cases the highest values of relative uncertainties are reported. Uncertainty for Pb is also substantial due to relatively small number of contributing sources. On the other hand, concentrations of NOx and PM_{10} in receptor 156 result from superposition of a large number of contributing sources (mostly areal but also neighboring linear sources) which implies relatively low uncertainties for both pollutants.

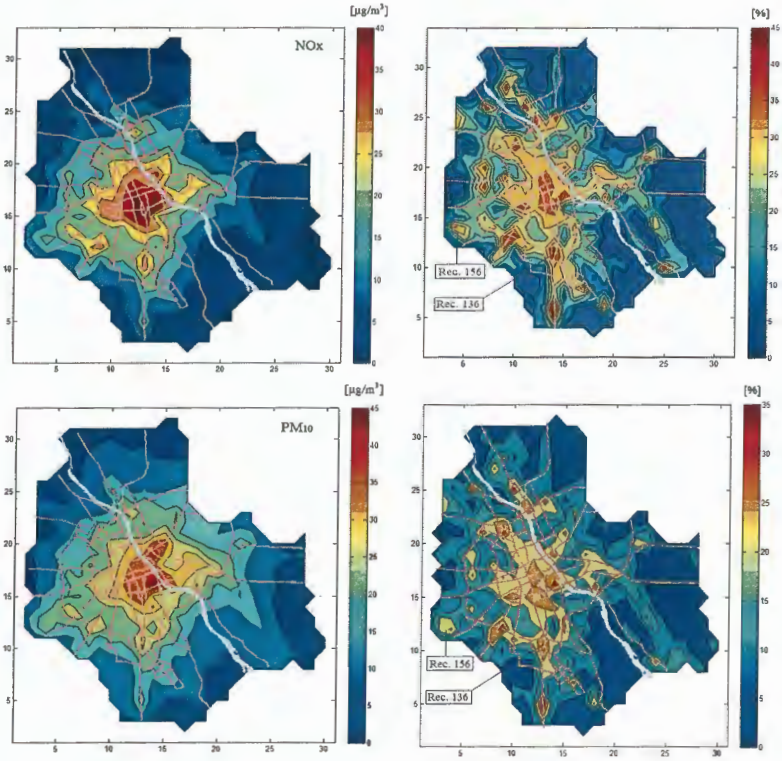

Fig. 7. Concentration (left) and relative uncertainty (right) for NOx (top), PM_{10} (bottom), and $PM_{2.5}$ (bottom).

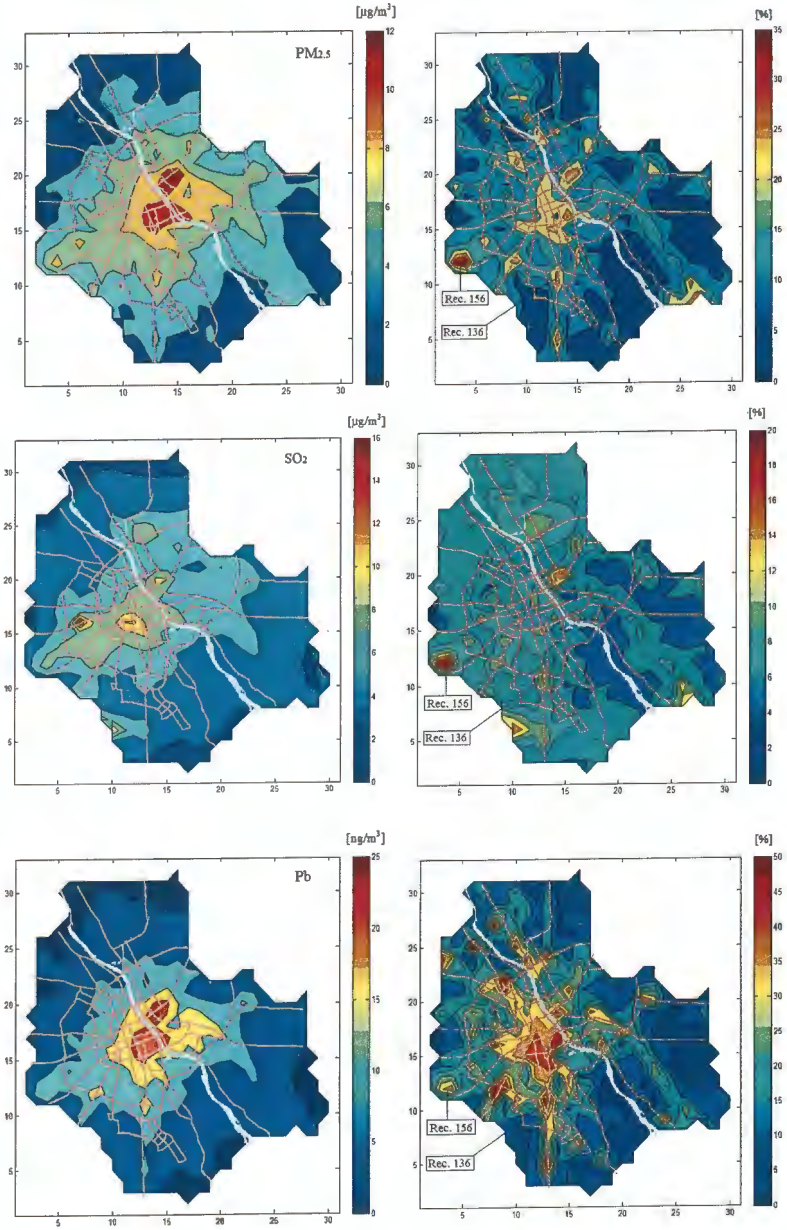

Fig. 7 (cont.) Concentration (left) and relative uncertainty (right) for $PM_{2.5}$ (top), SO_2 (middle) and Pb (bottom).

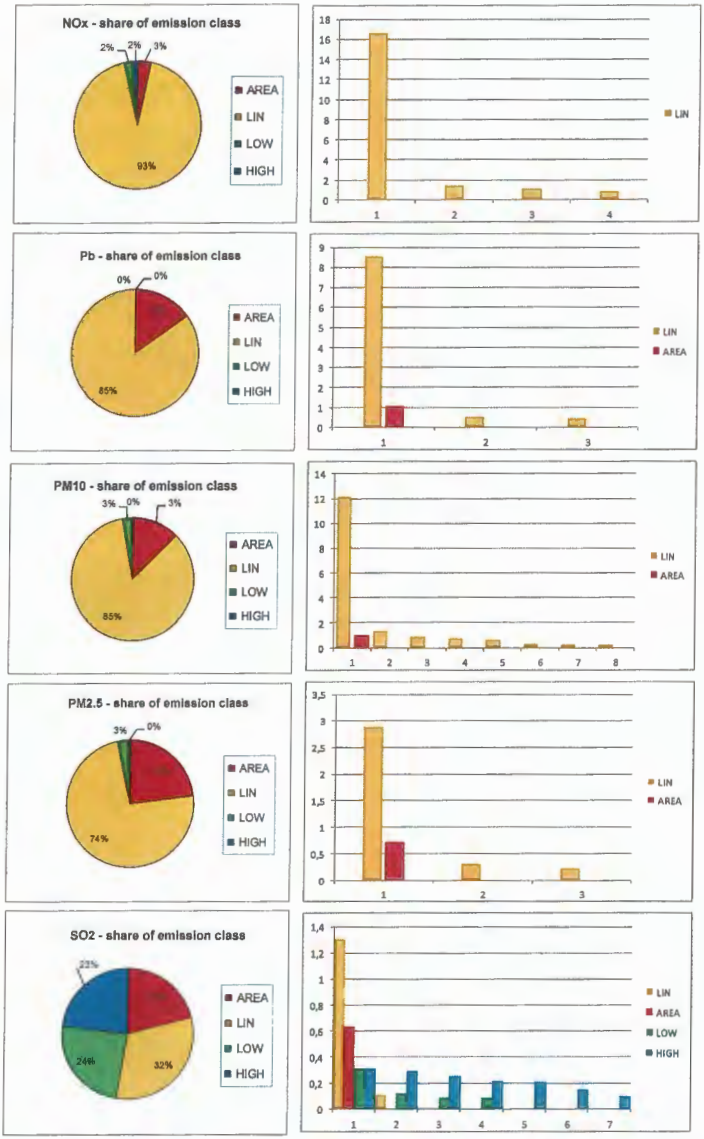

Fig. 8. Share of emission categories (left) and characteristics of sources (right) influencing different pollution types for the receptor 136, with noticeable dominating contributon of linear sources.

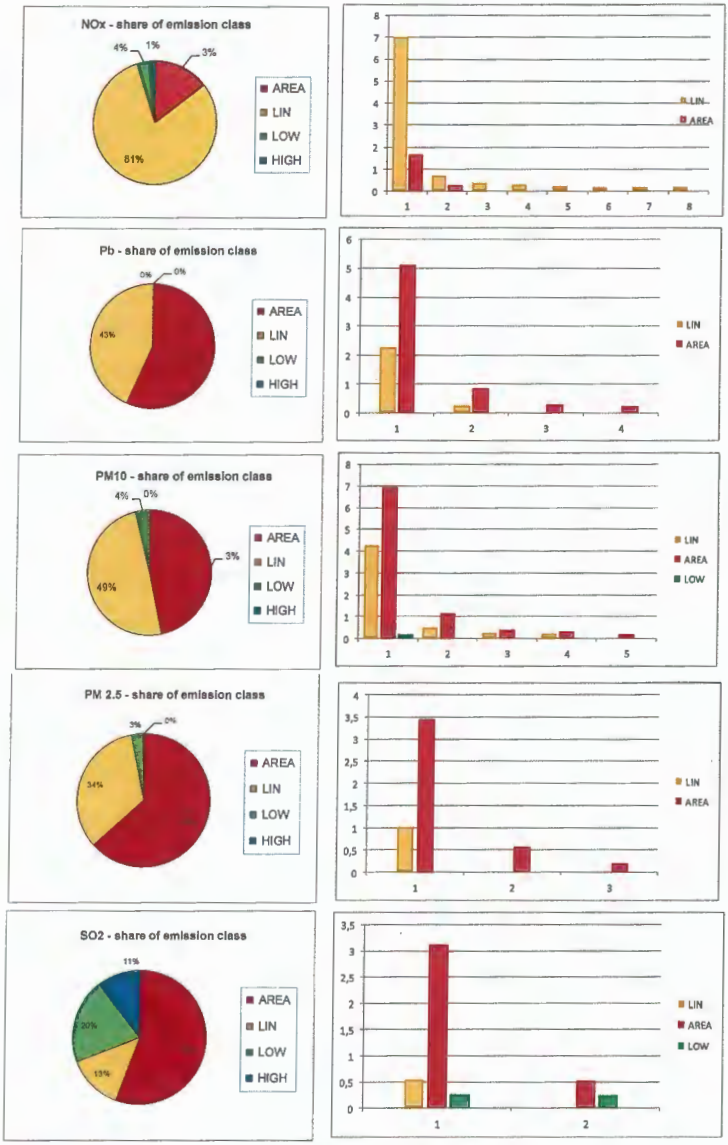

Fig. 9. Share of emission categories (left) and characteristics of sources (right) influencing different pollution types for the receptor 156,with noticeable dominating contribution of area sources.

5. Conclusions

This study presents selected results of computations related to modeling and uncertainty analysis of air pollution dispersion in the Warsaw Metropolitan Area. The analysis, dealing with the main urban-type polluting species, is based on the real meteorological data and emission field inventory for the year 2005. For the purpose of detailed, numerical procedure, the emission field was split down into four categories: (a) high point sources (power plants), (b) other point sources (industry), (c) area sources (residential sector), (d) linear sources (transportation). The main forecasting tool used in simulation of air pollution dispersion is the regional scale transport model CALPUFF (Scire et al., 2000). Linear structure of the model is utilized to calculate a polluting contribution of individual emission sources and to implement parallel computation for the purpose of Monte-Carlo algorithm and uncertainty analysis. The obtained results comprise the annual average concentrations of several polluting compounds, primary and secondary, which are characteristic for urban atmospheric environments. Results presented in the paper encompass mainly the sulfur and nitrogen oxide pollutants, lead, and particulate matter, PM_{10} and $PM_{2.5}$.

Secondary pollutants of $SO_4^{=}$ and NO_3^{-} have been taken into account in formation of the sulfate and nitrate aerosols, which are next included as components of particulate matter. Moreover, annual concentrations of Ni, Cd and BaP were computed, including their uncertainty assessments, but the analysis is omitted here due to the lack of representative set of the reference observation data.

The annual mean concentrations of sulfur dioxide in the urban domain are relatively low, and do not exceed air quality limits (critical level: 20 $\mu g/m^3$). The main sources, responsible for this type of pollution are power/heating plants, which are equipped with very high stacks (pollutants are mainly exported outside the urban area) and desulfurization installations. On the other hand, concentrations of particulate matter and nitrogen oxides are substantial and have a remarkable and negative impact on urban environment. Concentrations of NOx and PM_{10} are spatially strongly diversified, and reach very high values (especially in central

districts), which often exceed the critical values (critical levels: 30 $\mu g/m^3$ and 40 $\mu g/m^3$ for NOx and PM_{10}, respectively). The main source of this adverse environmental impact is the transportation system (including the transit traffic). New ring roads, which are now under construction, and displacement of the transit and heavy truck transport outside the central districts of the city, should improve the situation.

The main goal of the paper is analysis of spatial distribution of uncertainty of air quality forecast, induced by uncertainty of the emission dataset. It is shown that accuracy and uncertainty of air pollution forecast measured at any receptor point is directly related to the following three factors: (a) the kind of polluting compound considered, (b) the emission source category of the dominating contributor, and (c) the number of individual emission sources having a substantial share in the total pollution. The resulting uncertainty assigned to a receptor point decreases for growing number of contributing emission sources (the averaging effect). This fact is illustrated on two selected receptor points in the computational domain of the Warsaw Metropolitan Area.

For the air pollutants considered in this paper, relatively homogeneous distribution and low uncertainty applies to the concentrations of SO_2, which mainly depend on relatively precise input emission of point sources. On the other hand, very substantial uncertainties relate to NOx, PM_{10}, $PM_{2.5}$ and Pb forecasts, which strongly depend on the structure of contributing sources, with dominating impact of the urban transport. Moreover, very high spatial variability of uncertainty distribution, which is related to traffic-dependent pollutants was shown. Besides of the practicability of the above findings, general objectives of the presented uncertainty results are, as stated by Maxim & van der Sluijs (2011) to *bring scientific predictions closer to reality, increase decision maker's confidence of scientific results, improve stakeholder's and public's confidence in science, improve the quality of decisions.*

Acknowledgements

This project was supported by the by the Polish Ministry of Science and High Education under Grant NN519316735. We also thank Wojciech Trapp and the EKOMETRIA team for their assistance in emission data preparation.

References

ApSimon, H.M., Warren, R.F., Kayin S., 2002. Addressing uncertainty in environmental modeling: a case study of integrated assessment of strategies to combat long-range transboundary air pollution. *Atmospheric Environment,* 36, 5417–5426.

Buchholz, S., Krein, A., Junk, J., Heinemann, G., Hoffmann, L., 2013. Simulation of urban-scale air pollution patterns in Luxembourg: Contributing sources and emission scenarios. Environmental Modeling and Assessment, 18, 271–283.

Carnevale, C., Finzi, G., Pisoni, E., Volta, M., Guariso, G., Gianfreda, R., Maffeis, G., Thunis, P., White, L., Triacchini, G., 2012. An integrated assessment tool to define effective air quality policies at regional scale. Environmental Modelling & Software, 38, 306–315.

Calori, G., Clemente, M., De Maria, R., Finardi, S., Lollobrigida, F., Tinarelli, G., 2006. Air quality integrated modelling in Turin urban area. Environmental Modelling & Software, 21, 468–476.

Colvile, R.N., Woodfield, N.K., Carruthers, D.J., Fisher, B.E.A., Rickard, A., Neville, S., Hughes, A., 2002. Uncertainty in dispersion modeling and urban air quality mapping. Environmental Science & Policy, 5, 207–220.

Holnicki P., Nahorski, Z., Tainio, M., 2010. Uncertainty in air quality forecasts caused by emission uncertainty. Proceedings of HARMO 13th Conference on Harmonisation within Atmospheric Dispersion Modelling, 119 –123.

Holnicki, P., 2011. Uncertainty in integrated modeling of air quality. Advanced Air Pollution. INTECH Publishers, Rijeka, 239–260.

Jacobson, M.Z., 2005. Fundamentals of Atmospheric Modeling. Cambridge University Press, Cambridge, U.K.

Lim, L.L., Hughes, S.J., Hellawell, E.E., 2005. Integrated decision support system for urban air quality assessment. Environmental Modelling & Software, 20, 947–954.

Malherbe, L., Ung, A., Colette, A., Derby, E., 2011. Formulation and quantification of uncertainties in air quality mapping. ETC/ACM Technical Paper 2011/9, September 2011.

Maxim, L., van der Sluijs J., 2011. Quality in environmental science for policy: Assessing uncertainty as a component of policy analysis. Environmental Science & Policy, 14, 482–492.

Mediavilla-Sahagún, A., ApSimon, H.M., 2006. Urban scale integrated assessment for London: Which emission reduction strategies are more effective in attaining prescribed PM10 air quality standards by 2005? Environmental Modelling & Software, 21, 501–513.

Oxley, T., Valiantis, M., Elshkaki, A., ApSimon, H.M., 2009. Background, road and urban transport modeling of air quality limit values (The BRUTAL model). Environmental Modelling & Software 24, 1036–1050.

Page, T., Whyatt, J.D., Beven, K.J., Metcalfe, S.E., 2003: Uncertainty in modeled estimates of acid deposition across Wales: a GLUE approach. Atmospheric Environment, 38, 2079–2090.

Park, S.-K., Cobb, C.E., Wade, K., Mulholland, J., Hu Y., Russel, A.G., 2006. Uncertainty in air quality model evaluation for particulate matter due to spatial variations in pollutant concentrations. Atmospheric Environment, 40, S563–S573.

Russel, A., Dennis, D., 2000. NASTRO critical review of photochemical models and modeling. Atmospheric Environment, 34, 2283–2324.

Sax, T., Isakov, V., 2003. A case study for assessing uncertainty in local-scale regulatory air quality modeling applications. Atmospheric Environment, 37, 3481–3489.

Scire, J.S., Strimaitis, D.G., Yamartino, R.J., 2000. A User's Guide for the CALPUFF Dispersion Model. Earth Technology Inc.

Sportisse, B., 2007. A review of current issues in air pollution modeling and simulation. Computational Geosciences, 11, 159–181.

Tainio, M., 2009. Methods and uncertainties in the assessment of the health effects of fine particulate matter a (PM2.5) air pollution. National Institute for Health and Welfare, Research Report No 18, Helsinki, 165 pp.

Tainio, M., Tuomisto, J.T., Pekkanen, J., Karvosenoja, N., Kupiainen, K., Porvari, P., Sofiev, M., Karppinen, A., Kangas, L., Kukkonen, J., 2010. Uncertainty in health risks due to anthropogenic primary fine particulate matter from different source types in Finland. Atmospheric Environment, 44, 2115–2132.

Yang, J., 2011. Convergence and uncertainty analyses in Monte-Carlo based sensitivity analysis. Environmental Modelling & Software, 26, 444–1527.

Warmink, J.J., Janssen, J.A.E.B., Booij M.J., Krol, M.S., 2010. Identification and classification of uncertainties in the application of environmental models. Environmental Modelling & Software, 25, 1518–1527.